

FUZZY-BASED POSITIONING FOR MOBILE ROBOTS

Received 25th February 2009; accepted 12th March 2009.

Weimin Shen, Jason Gu, Max Meng

Abstract:

This paper proposes fuzzy-based positioning algorithms for an iRobot B21r mobile robot, which is equipped with a 180° scanning laser rangefinder and other sensors, in an indoor environment. A novel, dynamic error model for the laser rangefinder is built with consideration of the detection distance and the detection angle. A new concept, the virtual angular point, is introduced in this paper as one of the features for positioning a mobile robot. To position a mobile robot, three kinds of feature points, such as break points, real angular points, and virtual angular points, are employed in this paper. Based on fuzzy evaluation for the accuracy of each feature point, positions obtained by two arbitrary points are fused together by the weighted mean technique, in which weight is determined by the uncertainty represented by fuzzy numbers. Experimental study has been carried out to verify the effectiveness and the accuracy of the algorithms.

Keywords: position estimation, laser rangefinder, virtual angular points, fuzzy logic.

1. Introduction

Accurate perception of the position is essential in the application of a mobile robot. In particular, when a mobile robot is applied into autonomous tasks, it is required to know precisely where it is in order to navigate successfully to desired locations in its environment. This problem is the so-called “the first-location problem” [1]. Theoretical work, practical work, and different approaches on the subject have been reported, but it is still on the cutting-edge of research directions in the field of mobile robotics. Positioning of a mobile robot is the foundation for other application areas, such as trajectory planning [2], obstacle avoidance [3], and robot navigation [4].

Interaction between the mobile robot and objects in its surroundings is performed by using the interoceptive and exteroceptive sensors mounted on the mobile robot. To obtain the position of the mobile robot, many different sensors, systems, and techniques have been developed [5], [6], [7]. Traditionally, position feedback can be achieved through odometry sensors. It is the most widely used navigation method, since odometry provides good short-term accuracy, is inexpensive, and allows very high sampling rates. However, the fundamental idea of odometry is the integration of incremental motion information over time, which leads inevitably to the accumulation of errors that cause large position errors and increase proportionally with the distance traveled by the

robot [8]. Despite these limitations, most researchers agree that odometry is an important part of a robot navigation system, and that navigation tasks will be simplified if odometric accuracy can be improved [9], [10], [11]. Sonar sensors are also popular perception systems in mobile robotics. This kind of sensor has been used by various researchers [12], [13], [14], primarily due to their low cost and their ease of integration. Sonar sensors are based on a time-of-flight principle using an ultrasonic wave. Over the past decade, much research has been conducted investigating applicability in such areas as world modeling and collision avoidance, position estimation, and motion detection [15], [16], [17]. The major drawback of sonar sensors is the poor angular resolution due to the relatively large beam angle. In addition, the distance and spatial resolutions of sonar sensors are limited. They require significant post processing of data to provide accurate position updating [18]. As an alternative to the sonar sensors, the laser rangefinder is also a time-of-flight sensor that achieves significant improvements over the ultrasonic range sensor due to the use of laser light instead of sound. In recent years, the laser rangefinder has proved more popular in positioning mobile robots [19] and [20]. This is due to the fact that the laser rangefinder can provide dense data about the environment, so it is possible to extract suitable features from the reading of the laser rangefinder, and those features can be used for positioning a robot [21]. Vision systems are often used for recognition of landmarks in the environment [4], [22]. They are frequently used in a stereo vision head. Visual sensing provides a tremendous amount of information about a robot's environment, and it is potentially the most powerful source of information among all the sensors used on robots to date [23]. Due to the wealth of information, however, extraction of visual features for positioning is not an easy task and this method is hard to use in a real time application. Each sensor has its advantages and disadvantages. For different mobile robot tasks, different sensors are used. Sometimes, those sensors can be fused together to get more highly accurate positions.

Many techniques and methods are used for understanding the environment from sensor readings. Different solutions have been adopted in the robotics literature [24], [25], [26], [27]. In general, there are two approaches. One is the grid-based approach, and the other is the feature-based approach. The grid-based approach uses a 2D array to represent the environment. This low-level grid-based approach proves to be very useful for map building using ultrasonic sensors, because ultrasonic sensors have a large opening angle and their range

data are seriously corrupted by reflection. The feature-based approach represents the structure of the environment by geometrical primitives. They are represented by a set of parameters describing their shape, their position in the environment, and their position uncertainty. In the feature-based approach, the laser rangefinder scans are segmented into a set of features such as break points (a break point is defined as when the laser sensor reading is not continuous around it), corners or angular points (an angular point is defined as a transition point from one line to another line around which the data points are continuous), line segments, etc. There is a substantial body of previous research in the area of feature-based positioning by laser rangefinders [28], [29]. In [30], break points are used as the feature to position the mobile robot, however, they cannot provide an accurate position, because one pair of break points in separate scans are not at the same point in the environment. Other features such as corner points or line segments, have the same problem. With the increase in the detection distance and the decrease in the detection angle, errors in the laser rangefinder increase dramatically. One error model for the laser rangefinder in [1], the SP model, does not consider uncertainty changing due to the detection distance and the detection angle. To our knowledge, there is no published work to date developing an efficient method for positioning which takes into consideration of the detection distance and the detection angle. However, fuzzy logic can facilitate to describe uncertainties, such as big uncertainty, medium uncertainty, and small uncertainty. That is the reason why fuzzy logic is used in the paper to describe uncertainties of features.

The aim of this paper is to propose algorithms based on fuzzy logic to position the iRobot B21r mobile robot, which is equipped with a 180° scanning laser rangefinder and other sensors. The B21r mobile robot is ideal for research and development across a broad range of indoor robotics applications because it is easy to control and has various types of sensors, including inertial sensors, infrared sensors, tactile sensors, sonar sensors, a scanning laser rangefinder, and a stereo camera. However, the limitations of these sensors make obtaining a highly accurate position extremely challenging. In this paper, readings from the laser rangefinder and the inertial sensors will be fused together to get a precise position. The novelties of this research are a new error model for the laser rangefinder taking into consideration the detection distance and the detection angle, a new concept, the virtual angular point, and the position fusion technique based on the weighted mean technique and fuzzy uncertainty.

This paper is organized as follows. In Section 2, a novel error dynamic model for the laser rangefinder is put forward, including fuzzy-based error description for the features. Section 3 gives feature extraction algorithms and feature points pairing. Section 4 presents the positioning algorithms based on the weighted mean technique and fuzzy uncertainty. Section 5 details experiments designed to verify the effectiveness and accuracy of the method, and finally in Section 6 concluding remarks are discussed.

2. Laser rangefinder error model and Fuzzy Based Uncertainty Description

Typically, the model of a laser rangefinder with uncertainty regarding the detection distance and the scanning angle can be shown in Fig. 1. The uncertainty associated with the location of a 2D laser reading is represented, by the covariance matrix of its perturbation vector, where a zero-mean Gaussian error distribution is assumed [1]. In general, a scanning laser rangefinder collects scans, i.e., sets of m readings $\{\rho_i, \phi_i\}$, where ρ_i represents the detection distance to an object placed in the way of the laser beam in the direction determined by a scanning angle ϕ_i . The scanning angle takes m discrete values ranging from 0 to 180 degrees, so that $i = 1, \dots, m$, and $\Delta\phi = \phi_{i+1} - \phi_i = \text{const}$, and the indices i are additive modulo m .

Let α denote the angle between x axis and the target plane (as shown in Fig. 2), and β denote the detection angle (which is defined as the angle between the laser beam and the target plane, as shown in Fig. 2), so that we have, $\beta = \alpha - \phi_i$, which can be shown in Fig. 2. ρ_i will include large uncertainty at small values β , that is, at sharp angles of observation [31].

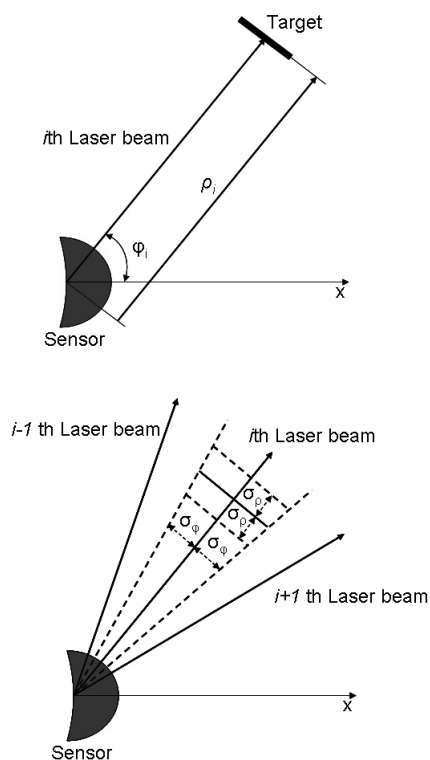


Fig. 1. Laser rangefinder model with uncertainty along to the detection angle and the detection distance.

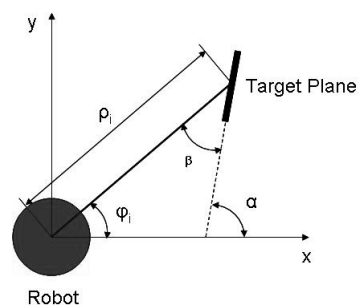


Fig. 2. The detection angle in the i th scan.

2.1. A Novel 2D Laser Rangefinder Error Model

In the feature-based approach, features are extracted from the laser rangefinder reading. These features could be line segments, corners, break points, etc. Fig. 3 gives an example of a 180° scanning of the gym at Sexton Campus. From this figure we can determine that laser rangefinder readings can be used to represent an indoor environment in the form of polygonal shapes.

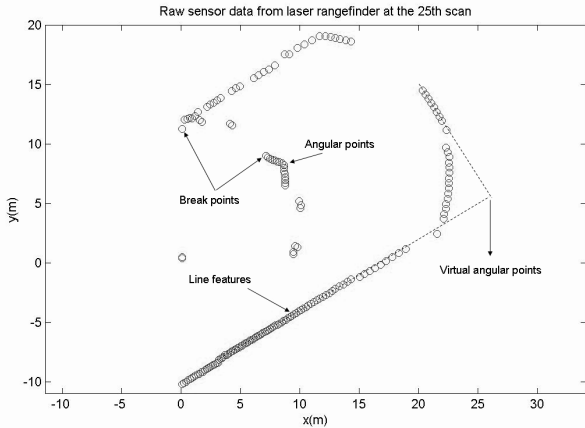


Fig. 3. Features in an 180° scanning set of the laser rangefinder reading.

It is obvious that break points, angular points, virtual angular points, and line segments can be used as features.

In an indoor environment, angular points could be the wall corner or the interfaces of objects with the wall. A break point can be defined as a point before or after a gap in the sequence of data points. Break points may locate at different positions in different laser scan when the robot moves. However, because of the uncertainty in the laser rangefinder, the same break points cannot be detected by the different scanning data; even a break point detected by the first scan cannot be detected by the second scan. As a result, break points can only provide rough information. The angular points have the same problem as the break points.

The virtual angular point refers to an intersectional point of two arbitrary lines. Virtual angular points do not exist in the real world and cannot be detected by the laser rangefinder. In general, we can get highly accurate slopes of line segments instead of the starting point, the ending point, and the length. More importantly, we can obtain some points with the short detection distance and the big detection angle, that is, the uncertainties in those points are very small, but they might only belong to one section of other feature segments, enabling us to continue using them for positioning in our algorithms. Using virtual angular points, we can get more accurate features to position a mobile robot. We know that the line segments have much more exact tangents than point features, due to a line including more points.

Because of light refraction noise and other variables, some points scanned by a laser rangefinder, which do not exhibit a local alignment within a tolerance, will be removed from the raw sensed data [32]. However, since the laser rangefinder has uncertainty itself as mentioned at the beginning of this section, there are two main reasons that will affect the laser rangefinder's accuracy,

as seen in Fig. 4. First, when the detection distance increases, the uncertainty of the laser rangefinder will increase accordingly. Second, when the detection angle is far from 90°, the readings of the laser rangefinder will contain large uncertainty for the discrete scanning. The uncertainty associated with the laser rangefinder is defined by:

$$\begin{cases} \alpha \propto |\beta - \pi/2| \\ \alpha \propto \rho \end{cases} \quad (1)$$

The relationship of the above equation is hardly represented by mathematic formulas, so fuzzy logic could be the best to represent this kind of uncertainty. In this paper, fuzzy logic is used to describe the uncertainty for the point, the virtual angular point, and the line feature (the line feature is defined as a sequence of points tracing out a line in the environment). Therefore, each feature is evaluated by fuzzy uncertainty. When the positions are fused, fuzzy uncertainty will be used as weights, namely, less uncertainty will have larger weight. By this way, the accuracy of position will be improved.

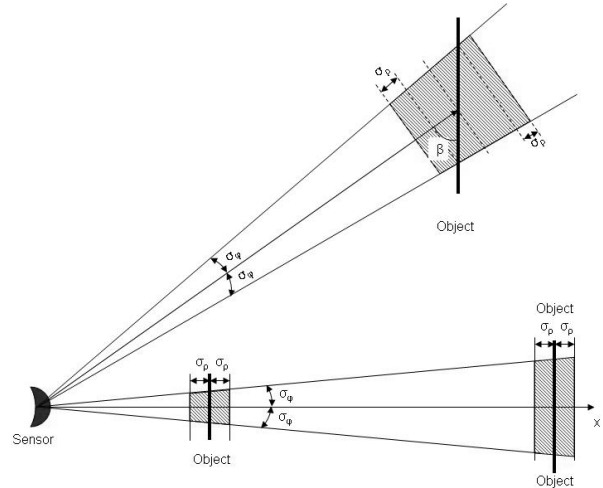


Fig. 4. Laser rangefinder scans the object, and there is uncertainty in laser reading (red area).

2.2. Fuzzy-Based Uncertainty Description for the Point Feature

Uncertainty of each point is determined by the fuzzy logic system with two inputs and one output. The two inputs are the detection distance and the detection angle, and the one output is the uncertainty associated with this point.

The reading matrix from a laser rangefinder is given by:

$$R_i = (\rho_i \quad \phi_i), i = 1, \dots, 180 \quad (2)$$

The detection distance between the laser rangefinder and the object can be obtained from the laser rangefinder reading directly. That is ρ_i .

The detection angle is formulated as:

$$\beta_i = \phi_i - \arctan\left(\frac{\rho_{i+1} \sin \phi_{i+1} - \rho_i \sin \phi_i}{\rho_{i+1} \cos \phi_{i+1} - \rho_i \cos \phi_i}\right) \quad (3)$$

The membership functions of those three variables, the detection distance, the detection angle, and the

uncertainty, are defined by triangular functions, because they only need vertex points to store them and thus to minimize the computer storage, and the sum of the triangular functions is equal to 1 that will simplify the expression. The membership functions are shown in Fig. 5, Fig. 6, and Fig. 7, respectively.

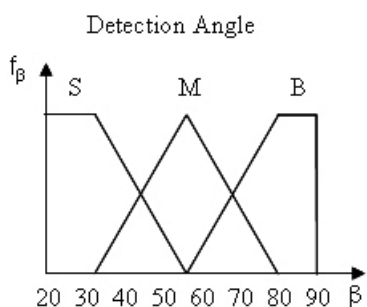


Fig. 5. The membership function of the detection angle.

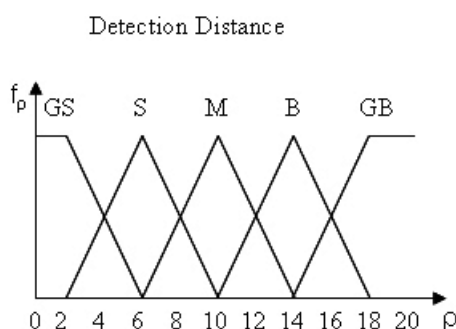


Fig. 6. The membership function of the detection distance.

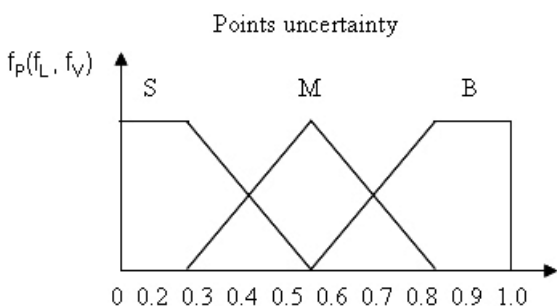


Fig. 7. Points Uncertainty.

The presented fuzzy logic decision system uses 15 rules, listed in Table 1. The proposed fuzzy logic decision system adopts the Mamdani-style inference engine and the max-min method for defuzzification.

Table 1. The fuzzy rules for accuracy estimation.

rho	beta		
	SMALL (S)	MEDIUM (M)	BIG (B)
GREAT SMALL (GS)	M	S	S
SMALL (S)	M	S	S
Medium (M)	B	M	M
Big (B)	B	B	M
Great Big (GB)	B	B	B

Therefore, the output of the uncertainty associated

with the point can be given by:

$$f_{pi}(\rho_i, \beta_i) = \frac{\sum_{l=1}^{15} \left[\frac{-|\rho - a_{\rho}^{l1}| + b_{\rho}^{l1}}{b_{\rho}^{l1}} \cdot \frac{-|\beta - a_{\beta}^{l1}| + b_{\beta}^{l1}}{b_{\beta}^{l1}} \right]}{\sum_{l=1}^{15} \left[\frac{-|\rho - a_{\rho}^{l1}| + b_{\rho}^{l1}}{b_{\rho}^{l1}} \cdot \frac{-|\beta - a_{\beta}^{l1}| + b_{\beta}^{l1}}{b_{\beta}^{l1}} \right]} \tag{4}$$

2.3. Fuzzy-Based Uncertainty Description for the Line Feature

In general, some methods are used for extracting the line feature from the laser rangefinder reading. After this processing, a series of points construct one line. The accuracy description regarding the raw points from the laser rangefinder reading can be obtained by the method mentioned in the above subsection. Still the fuzzy logic system is designed for describing the uncertainty of the line feature.

Generally, one line feature in a 2D environment can be expressed by:

$$a \cdot x + b \cdot y + c = 0 \tag{5}$$

There are two inputs, which are the mean of the uncertainty of points which construct the line feature, and the mean of distances between those points and the corresponding line feature.

The first input can be given by:

$$\delta = \frac{\sum_{i=1}^{m1} f_{pi}}{m1} \tag{6}$$

m1 is the number of points to construct the line.

The distance from a point to a line can be given by:

$$d_i = \left| \frac{x_i \cdot a + y_i \cdot a + c}{\sqrt{a^2 + b^2}} \right| \tag{7}$$

Therefore, the second input can be given by:

$$\sigma = \frac{\sum_{i=1}^{m1} d_i}{m1} \tag{8}$$

The membership functions of two input variables are defined by triangular functions by the same reasons mentioned in the above subsection, shown in Fig. 8 and Fig. 9, respectively. The membership function of the output is shown in Fig. 7.

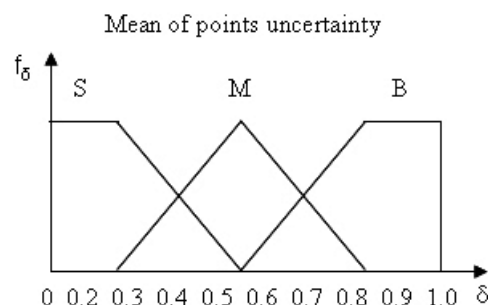


Fig. 8. The membership function of the mean of points accuracy.

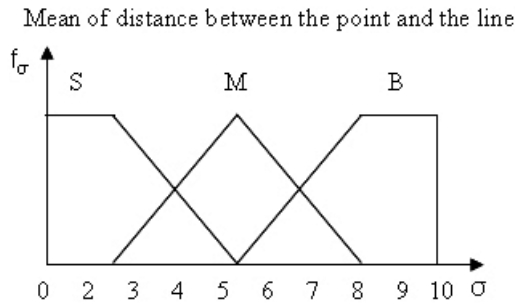


Fig. 9. The membership function of the mean of the distance between the point and the line.

The presented fuzzy decision system uses nine rules, listed in Table 2.

Table 2. The fuzzy rules for the line feature accuracy estimation.

	σ		
δ	SMALL (S)	MEDIUM (M)	BIG (B)
SMALL (S)	S	S	M
Medium (M)	S	M	B
Big (B)	M	B	B

By the same inference engine and defuzzification, the output of uncertainty can be given by:

$$f_{L1}(\delta, \sigma) = \frac{\sum_{l2=1}^{15} \left[\frac{y_L^{l2} \cdot \left(\frac{-|\delta - a_\delta^{l2}| + b_\delta^{l2}}{b_\delta^{l2}} \cdot \frac{-|\sigma - a_\sigma^{l2}| + b_\sigma^{l2}}{b_\sigma^{l2}} \right)}{\sum_{l2=1}^{15} \left[\frac{-|\delta - a_\delta^{l2}| + b_\delta^{l2}}{b_\delta^{l2}} \cdot \frac{-|\sigma - a_\sigma^{l2}| + b_\sigma^{l2}}{b_\sigma^{l2}} \right]} \right]}{(9)}$$

2.4. Fuzzy-Based Uncertainty Description for the Virtual Angular Points Feature

According to the definition of the virtual angular point, we know that two arbitrary lines can form one virtual angular point. So, the accuracy of virtual angular points depends on the accuracy of those two lines. Another property of such a point feature is that the small variation of the tangent of one line causes a big distance error if the point is far away from the central point of the line. It means that if the virtual angular point is too far away from the line segments, this point may be greatly inaccurate. Therefore, the uncertainty of the virtual angular points depends on three factors, two lines' uncertainty, and the distance between the virtual angular point and the center points of the line segments.

The first input and the second input can be obtained through the above subsection directly, denoted by f_{L1} and f_{L2} , respectively.

The third input is the mean of the distances between the virtual angular point and the center points of two line segments, which form the virtual angular point.

Let (x_v, y_v) denote the virtual angular point, and $(x_{c1}, y_{c1}), (x_{c2}, y_{c2})$ denote the center points of two line segments, respectively, then we have:

$$d_v = \frac{1}{2} \left(\sqrt{(x_v - x_{c1})^2 + (y_v - y_{c1})^2} + \sqrt{(x_v - x_{c2})^2 + (y_v - y_{c2})^2} \right) \quad (10)$$

The membership functions of the input variables are defined by triangular functions, as shown in Fig. 7 and Fig.10, respectively. The membership function of the output is shown in Fig. 7.

The mean of the distance between the virtual angular points and the center point of line

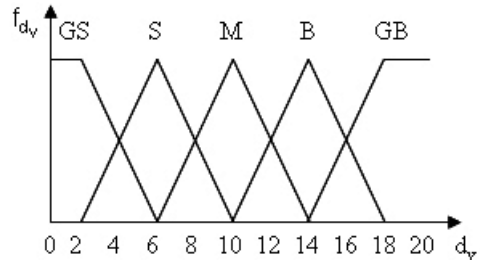


Fig. 10. The membership function of the mean of the distance between the point and the line.

The presented fuzzy decision system uses 45 rules, listed in Table 3.

By the same inference engine and defuzzification, the output of uncertainty can be given by:

$$f_v(f_{L1}, f_{L2}, d_v) = \frac{\sum_{l3=1}^{45} \left[\frac{y_v^{l3} f_{L1L2} \cdot \left(\frac{-|d_v - a_{dv}^{l3}| + b_{dv}^{l3}}{b_{dv}^{l3}} \right)}{\sum_{l3=1}^{45} \left[f_{L1L2} \cdot \frac{-|d_v - a_{dv}^{l3}| + b_{dv}^{l3}}{b_{dv}^{l3}} \right]} \right]}{(11)}$$

$$f_{L1L2} = \frac{-|f_{L1} - a_{fL1}^{l3}| + b_{fL1}^{l3} \cdot -|f_{L2} - a_{fL2}^{l3}| + b_{fL2}^{l3}}{b_{fL1}^{l3} \cdot b_{fL2}^{l3}} \quad (12)$$

Table 3. The fuzzy rules for the virtual angular point accuracy estimation.

	f_{L1}		
f_{L2}	SMALL (S)	MEDIUM (M)	BIG (B)
SMALL (S)	S	S	M
Medium (M)	S	M	B
Big (B)	M	B	B
$f_{L1} \cdot f_{L2}$			
d_v	SMALL (S)	MEDIUM (M)	BIG (B)
Great SMALL (GS)	S	S	M
SMALL (S)	S	S	M
Medium (M)	S	M	B
Big (B)	M	B	B
Great Big (GB)	B	B	B

3. Feature extraction and data association

The procedure for the mobile robot's feature extraction and points pairing includes the laser rangefinder reading filtering, which removes erroneous points and assigns the accuracy estimation for each point, finding break points, clustering, which classifies the points into several clusters, finding angular points, line feature extracting, finding virtual angular points, and points pairing, which is used for the positioning algorithm.

3.1. Filtering

Through the discussion of the above section, we know that the accuracy of laser rangefinder readings depends mainly on the detection distance, the detection angle, and the uncertainty associated with the sensor itself. Before the laser rangefinder reading is processed, it needs to remove some erroneous points, which have a very sharp detection angle. Assume that a point \mathbf{P}_i has a detection angle β_i . The rule for filtering is given by:

If $\beta_i \leq \xi_{TH}$, then \mathbf{P}_i is an erroneous point, this point needs to be removed.

where, ξ_{TH} is the threshold for the detection angle, we choose 22.5° in the paper. At the same time, as illustrated in Equation 4, each point will be assigned an uncertainty value in terms of the detection distance and the detection angle based on fuzzy logic.

3.2. Finding Break Points

Generally, in a total of 180 points of laser rangefinder reading per scan, break points are those points satisfying the following conditions.

$$\begin{cases} \|P_{i+1} - P_i - |P_{i-1} - P_i|\| > T_1, i = 2, \dots, 179 \\ |P_{i+1} - P_i| > T_2, & i = 2, \dots, 179 \\ \text{Break Points,} & i = 1, 180 \end{cases} \quad (13)$$

Where, $T_1; T_2$ are the threshold of the distance between two points.

3.3. Clustering

After break points are detected, the scan is broken at those points, thereby finding occlusions. The starting point and the ending point in one cluster should be break points. Line segments and angular points are classified into different clusters.

3.4. Finding Angular Points

Assume the current point \mathbf{P}_i needs to be checked. The angular points can be formulated as:

$$|\theta| \leq \theta_{TH}, 2 \leq i \leq 179 \quad (14)$$

Where, θ is the angle between $\mathbf{P}_{i-1}\mathbf{P}_i$ and $\mathbf{P}_i\mathbf{P}_{i+1}$ and θ_{TH} is the threshold of such an angle.

3.5. Line Feature Extraction

Line features are selected by determining the best fit for all points within the clustering segmented groups. This is accomplished in two steps: a) the least squares line fitting of each segmented group within a cluster, and b)

the computation of segment endpoints as the intersection points with neighboring line segments. The final result of this process is a set of line features (short ones in the case of non-structured environments) that approximate the contour of the surrounding obstacles.

3.6. Finding Virtual Angular Points

Arbitrarily, two lines with different tangents can form a virtual angular point, and those two lines are given by:

$$\begin{cases} y = a_1 \cdot x + b_1 \\ y = a_2 \cdot x + b_2 \end{cases} \quad (15)$$

Therefore, the intersectional point of those two lines can be obtained by:

$$\begin{cases} x = -\frac{b_2 - b_1}{a_2 - a_1} \\ y = -a_2 \cdot \frac{b_2 - b_1}{a_2 - a_1} + b_2 \end{cases} \quad (16)$$

However, the number of virtual angular points will increase dramatically as they appear on the intersection of every straight line in an environment with more straight edges. For this situation, we can still get good features of virtual angular points by fuzzy-based uncertainty description. For example, if the uncertainty for a virtual angular point is too big, this point will be removed. By this method, the number of virtual angular points will be decreased. Then, use well-chosen features to position the mobile robot by the weighted mean technique.

3.7. Data Association

Assume points in the i th scan and the $(i + 1)$ th scan are (x_{ki}, y_{ki}) , $(x_{k(i+1)}, y_{k(i+1)})$, respectively, where $k = 1, \dots, m$, which need to pair, and the increment of the inertial sensors is $(x_{0i}, y_{0i}, \theta_{0i})$. The strategy of pairing is first to map one point in the i th scan to the $(i + 1)$ th scan with the parameters obtained from the inertial sensors, second to find the point in the $(i + 1)$ th scan that is closest to this mapping point. If there is only one such point, then those two points are matched. We use the following homogenous transformation to map one point in the i th scan into the $(i + 1)$ scan:

$$\begin{bmatrix} x'_{ki} \\ y'_{ki} \\ \theta'_{ki} \end{bmatrix} = \begin{bmatrix} \cos \theta_{0i} & -\sin \theta_{0i} & x_{0i} \\ \sin \theta_{0i} & \cos \theta_{0i} & y_{0i} \\ 0 & 0 & 1 \end{bmatrix} \cdot \begin{bmatrix} x_{ki} \\ y_{ki} \\ \theta_{ki} \end{bmatrix} \quad (17)$$

Let d denote the distance between $(x_{k(i+1)}, y_{k(i+1)})$, and (x'_{ki}, y'_{ki}) , we have:

$$d = \sqrt{(x'_{ki} - x_{k(i+1)})^2 + (y'_{ki} - y_{k(i+1)})^2} \quad (18)$$

Therefore, if $d < T$, then (x_{ki}, y_{ki}) and $(x_{k(i+1)}, y_{k(i+1)})$ are one pair of points in the i th scan and $(i + 1)$ th scan, where T is the threshold of the distance.

4. Feature-based positioning for mobile robots

Any two pairs of points can position the robot. Use the following formulas to illustrate this point, shown in

Fig. 11. The expression of the transform matrix in the form of the homogeneous matrix is given by:

$$T = Trans(a, b)Rot(Z, \theta) = \begin{bmatrix} \cos \theta & -\sin \theta & a \\ \sin \theta & \cos \theta & b \\ 0 & 0 & 1 \end{bmatrix} \quad (19)$$

So that the relationship between one pair of points can be given by:

$$\begin{bmatrix} x_1 \\ y_1 \\ 1 \end{bmatrix} = T \cdot \begin{bmatrix} x'_1 \\ y'_1 \\ 1 \end{bmatrix} = \begin{bmatrix} \cos \theta & -\sin \theta & a \\ \sin \theta & \cos \theta & b \\ 0 & 0 & 1 \end{bmatrix} \cdot \begin{bmatrix} x'_1 \\ y'_1 \\ 1 \end{bmatrix} \quad (20)$$

The relationship between another pair of points can be obtained in the same manner, so we have:

$$\begin{bmatrix} x_1 \\ y_1 \\ x_2 \\ y_2 \end{bmatrix} = \begin{bmatrix} x'_1 & -y'_1 & 1 & 0 \\ y'_1 & x'_1 & 0 & 1 \\ x'_2 & -y'_2 & 1 & 0 \\ y'_2 & x'_2 & 0 & 1 \end{bmatrix} \cdot \begin{bmatrix} \cos \theta \\ \sin \theta \\ a \\ b \end{bmatrix} \quad (21)$$

So that:

$$\begin{bmatrix} \cos \theta \\ \sin \theta \\ a \\ b \end{bmatrix} = \begin{bmatrix} x'_1 & -y'_1 & 1 & 0 \\ y'_1 & x'_1 & 0 & 1 \\ x'_2 & -y'_2 & 1 & 0 \\ y'_2 & x'_2 & 0 & 1 \end{bmatrix}^{-1} \cdot \begin{bmatrix} x_1 \\ y_1 \\ x_2 \\ y_2 \end{bmatrix} \quad (22)$$

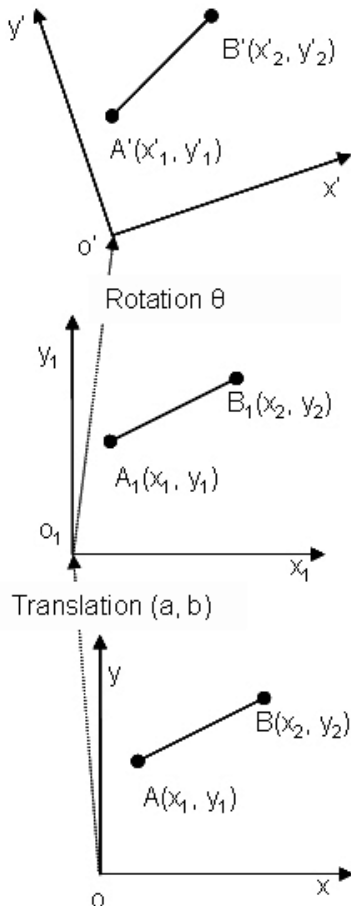


Fig. 11. Vector transformation with the translation $(a; b)$ and the rotation θ .

According to Equation 4, each point of break points and angular points has its fuzzy uncertainty description. The fuzzy uncertainty description for virtual angular points is given by Equation 11, which is determined by Equation 9. Assume that after points pairing, there are i pairs of break points, angular points, and virtual angular points, denoted by $\mathbf{P}_i = (p_{i1}, p_{i2})$, and fuzzy uncertainty associated with those points denoted by f_{i1} and f_{i2} , so that we can get the i th position from this pair of the points, and the accuracy associated with the i th position is given by:

$$f_i = \frac{f_{i1} + f_{i2}}{2} \quad (23)$$

Therefore, the position obtained from those pairs of points is denoted by (a_i, b_i, θ_i) . Total number of positions by paired points is denoted by $m2$. Then, the final position is fused by:

$$a = \frac{\sum_{i=1}^{m2} a_i f_i}{\sum_{i=1}^{m2} f_i}, b = \frac{\sum_{i=1}^{m2} b_i f_i}{\sum_{i=1}^{m2} f_i}, \theta = \frac{\sum_{i=1}^{m2} \theta_i f_i}{\sum_{i=1}^{m2} f_i} \quad (24)$$

5. Experiments

The iRobot B21r mobile robot is an indoor mobile robot system developed by iRobot Corporation. The mobile robot possesses a synchronized drive mode with four steer- and drive-wheels, achieving a maximum speed of 1m/s. An on-board host computer implements the control software required to control both the internal navigation parameters of the vehicle and the interaction of the mobile robot with its surrounding environment using its exteroceptive sensors. The mobile robot is equipped with incremental encoders which return the rotation angle of the wheel, from which an estimation of the relative displacement of the vehicle can be obtained. The exteroceptive sensors mounted on the robot are: a sonar ring, formed by 48 Polaroid ultrasonic sensors, which return distance information from the surrounding obstacles; a binocular stereo rig, formed by two off-the-shelf CCD cameras; and a laser rangefinder which delivers accurate, low noise range information from an actively scanned infrared laser beam.

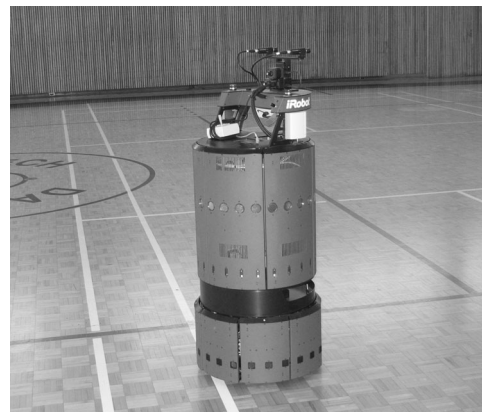


Fig. 12. iRobot running in the gym.

The mobile robot was programmed to follow a circle in the gym at Sexton Campus, which is shown in Fig. 12.

Why we choose a circle curve is that it is a typical and effective curve to reflect the slippage and integration drifting phenomena in a mobile robot. Suppose that the conditions of the floor are the same everywhere. We define the starting point and measure the ending point. Because of the evenly slippery floor, the actual path of the mobile robot is a spiral curve. Therefore, by the starting point and the ending point, the actual path can be calculated.

The laser rangefinder reading is filtered, so that incorrect points are removed and other points are assigned uncertainty values. The filtering result of the 25th scan is shown in Fig 13. Based on the break points finding algorithms, the break points in the 25th scan are found and shown in Fig. 14. Fig. 15 shows the angular points finding result in the 25th scan. The 25th scan is classified into 10 clusters, as shown in Fig. 16. Line features, which are shown in Fig. 17, are found in the 25th scan. Here, only lines which have at least four points are picked, because they are useful to decrease the complexity in finding the virtual angular points. Virtual angular points are found and shown in Fig. 18. Finally, the position estimation is calculated, shown in Fig. 19 and Fig. 20. From this figure, in the short distance, the inertial sensors can give high accuracy, and the position given by the inertial sensors is better than that of the algorithms in the paper, but with the increasing in distance, the inertial sensors contain large errors in the position, so that the algorithms in the paper is much better than the odometry method.

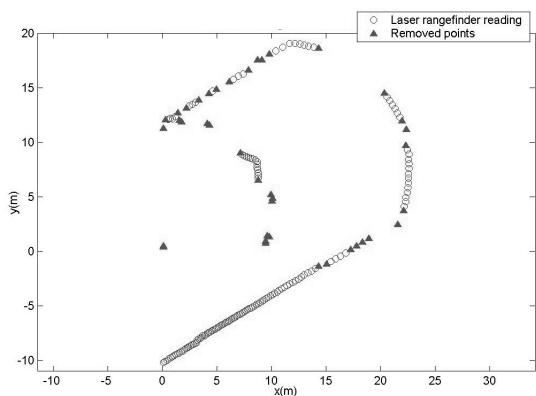


Fig. 13. Data filtering at 25th scan.

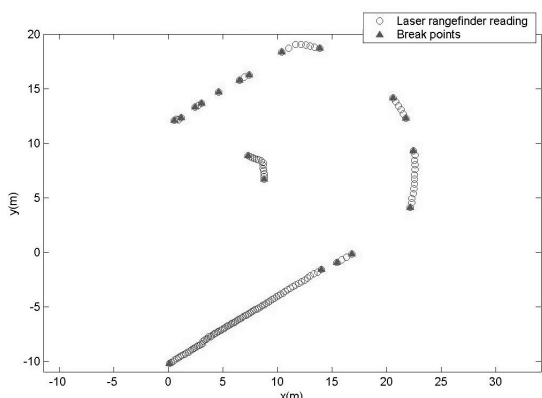


Fig. 14. Break points finding at 25th scan.

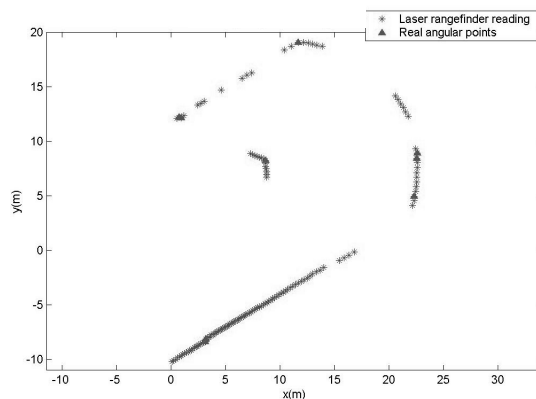


Fig. 15. Angular points finding at 25th scan.

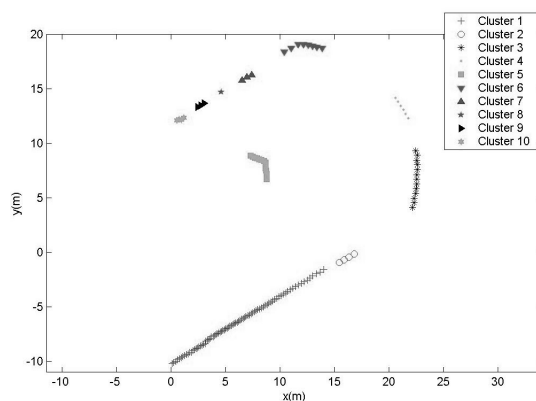


Fig. 16. Data clustering.

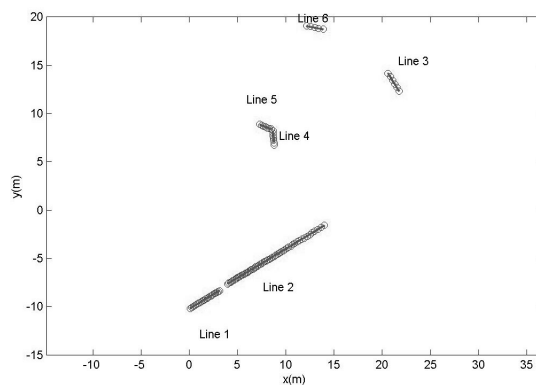


Fig. 17. Line features extracting at the 25th scanning.

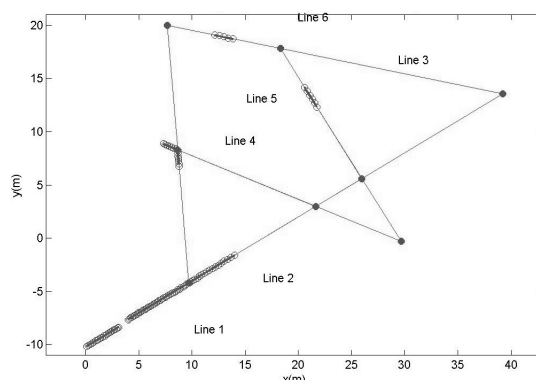


Fig. 18. Virtual angular points finding at the 25th scanning.

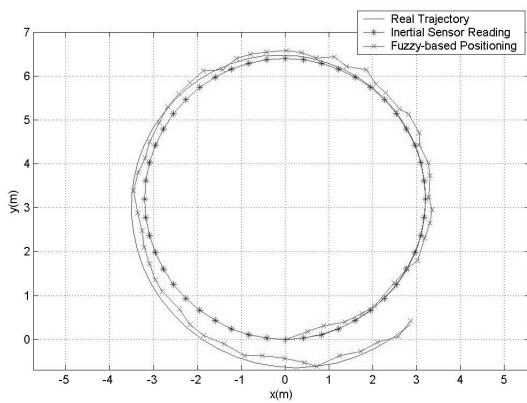


Fig. 19. The Comparison of the real trajectory, inertial sensor reading, and fuzzy-based positioning.

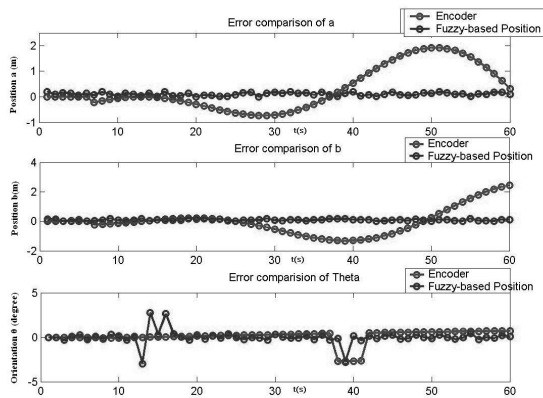


Fig. 20. The Comparison of the real trajectory, inertial sensor reading, and fuzzy-based positioning.

6. Conclusion and future work

In this paper, the proposed research built a new dynamic error model with consideration of the detection distance and the detection angle. A new concept, "virtual angular point", was defined and used for positioning. Fuzzy-based weight mean position fusion was presented. The procedure for positioning was put forward. The proposed research achieved significant improvement for the mobile robot positioning. The procedure of our positioning can be discussed as follows.

1. Before processing the laser rangefinder reading, it is important to filter data. It can decrease complexity of the whole positioning, and improve accuracy. Through fuzzy-based uncertainty descriptions, it is easy and efficient to present the uncertainty associated with laser measurement.
2. Virtual angular points have higher accuracy than break points and angular points. It is an innovative method to map the two different coordinate frames.
3. During the phase of fusing break points, angular points, and virtual angular points, the fuzzy method was implemented to decide weighted coefficients for corresponding data, then to obtain the weighted mean position and orientation of the mobile robot. This intuitive method can be easily understood, and the uncertainty is simple to express.

Although the experiment setting is a little simple, the complicated environment and obstacles in the environment will be considered in the future work.

AUTHORS

Weimin Shen* - Department of Electrical and Computer Engineering, Dalhousie University, Halifax, B3J 1Z1, Canada. E-mail: weimin.shen@dal.ca.

Jason Gu - Department of Electrical and Computer Engineering, Dalhousie University, Halifax, B3J 1Z1, Canada. E-mail: Jason.Gu@dal.ca.

Max Meng - Department of Electronic Engineering, The Chinese University of Hong Kong, Shatin, N. T., Hong Kong. E-mail: max@ee.cuhk.edu.hk.

* Corresponding author

References

- [1] Castellanos J.A., Tardos J.D., *Mobile robot localization and map building: a multi-sensor fusion approach*, Kluwer Academic Publishers: Massachusetts, 1999.
- [2] Kunwar F., Benhabib B., "Rendezvous-Guidance Trajectory Planning for Robotic Dynamic Obstacle Avoidance and Interception", *IEEE Transactions on Systems, Man, and Cybernetics - Part B: Cybernetics*, vol. 36, no. 6, 2006, pp. 1432-1441.
- [3] Diaz de León J.L., Sossa J.H., "Automatic Path Planning for a Mobile Robot Among Obstacles of Arbitrary Shape", *IEEE Transactions on Systems, Man, and Cybernetics - Part B: Cybernetics*, vol. 28, no. 3, 1998, pp. 467-472.
- [4] DeSouza G.N., Kak A.C., "Vision for Mobile Robot Navigation: A Survey", *IEEE Transactions on Pattern Analysis and Machine Intelligence*, vol. 24, no. 2, 2002, pp. 237-267.
- [5] Borenstein J., Everret H.R., Feng L., Wehe D., "Mobile Robot Positioning Sensors and Techniques", the *Journal of Robotic Systems*, vol. 14, no. 4, 1997, pp. 213-249.
- [6] Skrzypczynski P., "On Qualitative Uncertainty in Range Measurements from 2D Laser Scanners", *Journal of Automation, Mobile Robotics and Intelligent Systems*, vol. 2, no. 2, 2008, pp. 35-43.
- [7] Lee H., Kim M.N., Cho H., "A New 3D Sensor System by Using Virtual Camera Model and Stereo Vision for Mobile Robots", *Journal of Automation, Mobile Robotics and Intelligent Systems*, vol. 2, no. 4, 2008, pp. 38-44.
- [8] Everett H.R., *Sensors for mobile robots: theory and application*. A K Peters: Massachusetts, 1995.
- [9] Martinelli A., "The Odometry Error of a Mobile Robot with a Synchronous Drive System", *IEEE Transactions on Robotics and Automation*, vol. 18, no. 3, 2002, pp. 399-405.
- [10] Borenstein J., "Experimental Results from Internal Odometry Error Correction with the OmniMate Mobile Robot", *IEEE Transactions on Robotics and Automation*, vol. 14, no. 6, 1998, pp. 963-969.
- [11] Siemiątkowska B., Gnatowski M., Zychewicz A., "Fast Method of 3D Map Building Based on Laser Range Data", *Journal of Automation, Mobile Robotics and Intelligent Systems*, vol. 1, no. 2, 2007, pp. 35-39.
- [12] Wijk O., Christensen H.I., "Triangulation-based Fusion

- of Sonar Data with Application in Robot Pose Tracking", *IEEE Transaction on Robotics and Automation*, vol. 16, no. 6, 2000, pp. 740-752.
- [13] Kuc R., Barshan B., "Bat-Like Sonar for Guiding Mobile Robots", *IEEE Control Systems Magazine*, vol. 12, no. 4, 1992, pp. 4-12.
- [14] Brudka M., Pacut A., "Intelligent Robot Control Using Ultrasonic Measurements", *IEEE Transactions on Instrumentation and Measurement*, vol. 51, no. 3, 2002, pp. 454-459.
- [15] Ohya I., Kosaka A., Kak A., "Vision-Based Navigation by a Mobile Robot with Obstacle Avoidance Using Single-Camera Vision and Ultrasonic Sensing", *IEEE Transactions on Robotics and Automation*, vol. 14, no. 6, 1998, pp. 969-978.
- [16] Tsai C., "A Localization System of a Mobile Robot by Fusing Dead-Reckoning and Ultrasonic Measurements", *IEEE Transactions on Instrumentation and Measurement*, vol. 47, no. 5, 1998, pp. 1399-1404.
- [17] Gutierrez-Osuna R., Janet J.A., Luo R.C., "Modeling of Ultrasonic Range Sensors for Localization of Autonomous Mobile Robots", *IEEE Transactions on Industrial Electronics*, vol. 45, no. 4, 1998, pp. 654-666.
- [18] Song K.T., Tang W.H., "Environment perception for a mobile robot using double ultrasonic sensors and a CCD camera", *IEEE Transactions on Industrial Electronics*, vol. 43, no. 3, 1996, pp. 372-379.
- [19] Srinivasan V., Lumia R., "A pseudo-interferometric laser range finder for robot applications", *IEEE Transactions on Robotics and Automation*, vol. 5, no. 1, 1989, pp. 98-105.
- [20] Larsson U., Forsberg J., Wernersson A., "Mobile robot localization: integrating measurements from a time-of-flight laser", *IEEE Transactions on Industrial Electronics*, vol. 43, no. 3, 1996, pp. 422-431.
- [21] Gamini Dissanayake M.W.M., Newman P., Clark S., Durrant-Whyte H.F., Csorba M., "A solution to the Simultaneous Localization and Map Building (SLAM) Problem", *IEEE Transaction on Robotics and Automation*, vol. 17, no. 3, 2001, pp. 229-241.
- [22] Schmitt T., Hanek R., Beetz M., Buck S., Radig B., "Cooperative probabilistic state estimation for vision-based autonomous mobile robots", *IEEE Transactions on Robotics and Automation*, vol. 18, no. 5, 2002, pp. 670-684.
- [23] Baumgartner E.T., Skaar S.B., "An autonomous vision-based mobile robot", *IEEE Transactions on Automatic Control*, vol. 39, no. 3, 1994, pp. 493-502.
- [24] Georgiev A., Allen P.K., "Localization methods for a mobile robot in urban environments", *IEEE Transactions on Robotics and Automation*, vol. 20, no. 5, 2004, pp. 851-864.
- [25] Briechle K., Hanebeck U.D., "Localization of a mobile robot using relative bearing measurements", *IEEE Transactions on Robotics and Automation*, vol. 20, no. 1, 2004, pp. 36-44.
- [26] Lee J.M., Son K., Lee M.C., Choi J.W., Han S.H., Lee M.H., "Localization of a mobile robot using the image of a moving object", *IEEE Transactions on Industrial Electronics*, vol. 50, no. 3, 2003, pp. 612-619.
- [27] R. Talluri, J.K. Aggarwal, "Position estimation for an autonomous mobile robot in an outdoor environment", *IEEE Transactions on Robotics and Automation*, vol. 8, no. 5, 1992, pp. 573-584.
- [28] Barber R., Mata M., Boada M.J.L., Armingol J.M., Salichs M.A., "A Perception System based on Laser Information for Mobile Robot Topologic Navigation". *Proceedings of the 2002 28th Annual Conference of the IEEE Industrial Electronics Society (IECON 02)*, vol. 4, Spain, November 2002, pp. 2779-2784.
- [29] Lionis G.S., Kyriakopoulos K.J., "A Laser Scanner based Mobile Robot SLAM Algorithm with Improved Convergence Properties", *Proceedings of the 2002 IEEE/RSJ International Conference on Intelligent Robots and Systems*, Lausannem, Switzerland, October 2002, pp. 582-587.
- [30] Zhou X.W., Ho Y.K., Chua C.S., Zou Y., "The Localization of Mobile Robot Based on Laser Scanner", *2000 Canadian Conference on Electrical and Computer Engineering*, vol. 2, Halifax, March 2000, pp. 7-10.
- [31] Dubrawski A., Siemiatkowska B., "A Method for Tracking Pose of a Mobile Robot Equipped with a Scanning Laser Rangefinder", *Proceedings of the 1998 IEEE International Conference on Robotics and Automation*, Leuven, Belgium, May 1998, pp. 2518-2523.
- [32] Gonzalez J., Ollero A., Reina A., "Map Building for a Mobile Robot Equipped with a 2D Laser Rangefinder", *1994. IEEE International Conference on Robotics and Automation*, May 1994, pp. 1904-1909.